Deep Resources Engineering 2 (2025) 100187

Contents lists available at ScienceDirect

Deep Resources Engineering

journal homepage: www.keaipublishing.com/en/journals/deepre/

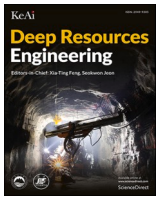

Generation of and countermeasures against time-delayed rockbursts

Ben-Guo He [a,b,*], Hong-Pu Li [a,b], Xia-Ting Feng [a,b], Zi-Hui Zhu [a,b], Han-Yi Liu [a,b], Heng-Yuan Zhang [a,b], Xiang-Rui Meng [a,b]

[a] State Key Laboratory of Intelligent Deep Metal Mining and Equipment, Northeastern University, Shenyang 110819, China
[b] Key Laboratory of Liaoning Province on Deep Engineering and Intelligent Technology, Northeastern University, Shenyang 110819, China

ARTICLE INFO

Keywords:
Time-delayed rockburst
Wave-absorbed technology
In-situ stress
Geological structure
Dynamic disturbance

ABSTRACT

Time-delayed rockbursts abruptly release huge energy, characterized by suddenness, randomness, and destructiveness, leading to substantial damage to both lives and property. This study explores the occurrence of time-delayed rockbursts through statistical analysis of case studies in deep tunnels, including an extremely intensive time-delayed rockburst case. Through on-site surveys, blasting vibration tests, numerical calculations, and true triaxial compression experiments, this study analyzes the main factors and prevention and control strategies of time-delayed rockbursts based on an extremely intense time-delayed rockburst case. The results show that most time-delayed rockbursts are of high intensity. Paramount factors influencing their occurrence consider *in-situ* stresses, structural planes, and dynamic disturbances. Both high *in-situ* stress and its gradients provide the necessary conditions for such events, while the presence of abundant structural planes and frequent dynamic disturbances largely increase the risk of rockburst potential. To mitigate the risk of time-delayed rockbursts, energy control strategies are essential, incorporating measures such as energy reduction, prerelease, energy transformation, and energy absorption. Additionally, wave-absorbed support technology can reduce the amplitude and frequency of dynamic disturbances, further decreasing the likelihood of a rockburst occurring. Time-delayed rockburst occurrence requires long disturbance durations, compared to immediate rockbursts. Long-term, continuous, and multiple dynamic events will cause significant damage accumulation and formation of microcracks in hard rock. This study offers insights into the mechanisms underpinning time-delayed rockbursts and proposes prevention strategies for their control.

1. Introduction

Rockbursts are a common occurrence in underground excavations, such as those for water conservancy and hydropower projects, traffic tunnels, deep mining, and underground laboratories [9]. These events, which are a major focus in the field of rock mechanics [14,15], are generally classified into immediate, time-delayed, and intermittent types based on their temporal and spatial characteristics [6]. Time-delayed rockbursts, which occur days to months after excavation, are particularly unpredictable and destructive, often causing significant damage without obvious precursors [3]. For example, during the construction of the Jinping II Hydropower Station diversion tunnel, a severe time-delayed rockburst occurred in the tunnel section K11 + 070 to K11 + 006 [26]. The shockwave from the event caused a construction vehicle involved in muck removal to rotate 90° and sustain severe damage, leading to its scrapping and several days of work stoppage, as well as significant loss of life and property. This incident highlighted the challenges of engineering design, construction, and disaster prevention in such environments.

A rockburst is a dynamic phenomenon characterized by the sudden release of accumulated elastic strain energy in rock masses, typically triggered by excavation or other external factors in high-stress areas [20]. This release results in the fracturing and ejection of surrounding rock, making rockbursts sudden, random, and highly damaging. Time-delayed rockbursts occur after stress adjustment and rebalancing following excavation unloading in deep tunnels. Due to their high randomness in location and timing, these events are difficult to predict and often lead to catastrophic impacts. Time-delayed rockbursts can be further categorized into spatial-temporal delayed and time-delayed types [8,26]. Spatial-temporal delayed rockbursts occur outside the stress adjustment disturbance range, a certain distance behind the tunnel face, after some time following excavation. Time-delayed rockbursts occur within the stress adjustment

* Corresponding author at: State Key Laboratory of Intelligent Deep Metal Mining and Equipment, Northeastern University, Shenyang 110819, China.
E-mail address: hebenguo@mail.neu.edu.cn (B.-G. He).

https://doi.org/10.1016/j.deepre.2025.100187
Received 22 August 2024; Received in revised form 11 April 2025; Accepted 30 April 2025
Available online 4 May 2025

range but after a delay, typically when excavation at the tunnel face is slow or has stopped for a period. The criteria for distinguishing between these two types are summarized in Table 1.

A large amount of time-delayed rockbursts have been identified based on the collected cases of rockbursts from Jinping II Hydropower Station diversion tunnel, Qinling Tunnel No. 4 diversion tunnel, Ping'an Tunnel, Lujialing Tunnel, Taipingyi Hydropower Station No. 2 diversion tunnel, and Paomashan No. 2 tunnel. Furthermore, the intensity grade is predominantly strong when time-delayed rockbursts occur. For instance, Jinping II Hydropower Station diversion tunnel experienced 44 time-delayed rockbursts, with 43 intensive time-delayed rockbursts and one moderate rockburst. A tunnel in south-west China also underwent high intensity time-delayed rockbursts, with the right-hand tunnel undergoing five rockbursts that damaged the steel arches, and the left-hand tunnel experiencing 15 incidents that repeatedly damaged steel arches, excavators, and other equipment. On April 8, 2022, an intensive spatial-temporal delayed rockburst occurred 30–80 m behind the tunnel face, with a crater length of approximately 40 m and a crater depth of 2–3 m, distributed within a 120° range at the arch (Fig. 1).

Numerous investigations have been conducted on the mechanisms, prediction, and prevention and control aspects of rockbursts [1,21,25]; however, most studies primarily focused on immediate rockburst [2,25], the research about time-delayed rockbursts remains unclear. Feng et al. [6] investigated the mechanisms and processes of a strainburst, strain-structural plane slip rockburst, immediate rockburst, and a time-delayed rockburst based on an analysis of microseismic activity therein. Su et al. [22] conducted extensive true triaxial tests to investigate the effect of dynamic disturbances on inducing time-delayed rockbursts. He et al.[13] examined the relationship between different stress states and rockburst induction, considering both static and dynamic stress conditions in the surrounding rock after tunnel excavation [18]; they also introduced a novel energy-absorbing bolt. In the field of rockburst prevention and control, researchers have developed numerous energy-absorbing bolts [4,12], some of which have been applied in hard rock mines, tunnels, and other underground engineering prone to rockburst. Despite significant progress in the study of time-delayed rockburst through extensive research efforts, the complex factors and conditions involved, along with the limited effective monitoring range of microseismic equipment [16]. Moreover, time-delayed rockbursts are characterized by massive energy release, high unpredictability, randomness, and destructiveness [10,17], suggesting that merely enhancing the strength of the supports may not suffice for effective control. Therefore, understanding the mechanism underpinning a time-delayed rockburst, mastering its evolution, predicting its occurrence, and determining effective preventative measures remain difficult.

Based on statistical data from numerous time-delayed rockburst cases, a typical extremely intensive time-delayed rockburst case was analyzed. On-site geological surveys, blasting vibration monitoring, *in-situ* stress inversion, and true triaxial compression tests were used in the analysis. Three key factors contributing to time-delayed rockbursts were identified. It also presents the principles and methods of energy control for preventing and controlling time-delayed rockbursts, and introduces a structurally simplified stepwise decoupling energy-absorbed and shock-absorbed bolt to control the hazards of rock ejecta impact, which provides valuable assistance for the prediction and prevention of time-delayed rockbursts.

Table 1
Criteria for distinguishing between spatial-temporal delayed and time-delayed rockbursts (after Feng et al. [8]; Zhang et al. [26].

Types of time-delayed rockburst	Occurrence time	Occurrence locations
Time delayed	Delay behind the working face by up to 18 days	Occur within 30 m behind the working face
Spatial-temporal delayed	Delay mainly within 10–30 days, with the majority within 80 days	Occur within 30–80 m behind the working face, with the majority within 400 m.

Fig. 1. Intensive spatial-temporal delayed rockburst in a tunnel in south-west China.

2. Engineering background

The extremely intensive time-delayed rockburst case occurred in the inclined shaft project of a deeply buried tunnel in southwest China. The research zone is located in the region with the most intense geological tectonic movement in China. Under the influence of tectonic stress, the elevation is continuously increasing, with the highest point in the region reaching 6000 m. The tunnel is near the Dadu River, where the rugged terrain and deep, rapidly incised valley create a prominent stress field, with locally high stress. The tunnel excavation zone is located in the influence zone of a "V"-shaped river valley, where the relative elevation difference exceeds 1000 m, and the maximum incision depth of the valley can reach 2000 m. The geographical location and topography of the tunnel are shown in Fig. 2a. The inclined shaft outlet is located in the "V"-shaped river valley, with a maximum burial depth of about 1621 m. The cross-sectional dimensions of the inclined shaft are 7.5 m × 7.5 m (width × height), as shown in Fig. 2b. Drilling and blasting methods are used for excavation, with a full-face excavation plan.

An extremely intense time-delayed rockburst, known as the "9.21" rockburst, occurred in the inclined shaft. The rockburst occurred in a tunnel section with Class III surrounding rock, approximately 150 m from the left gully center and at a depth of 280 m. The cross-section exhibited a significant height difference, being lower on the left and higher on the right. The affected area of the rockburst spanned 51 m in length, with a maximum depth of approximately 5 m and a volume of about 150 m^3. The rockburst center was 630 m from the tunnel face, and the rockburst occurred more than 100 days after excavation. This is a typical extremely intensive spatial-temporal delayed rockburst, as depicted by the rockburst photograph at the site shown in Fig. 2c.

3. Main factors influencing time-delayed rockbursts

After excavation, the stress in the surrounding rock gradually stabilizes, but the surrounding rock under long-term high-stress conditions undergoes creep deformation. During the creep process, rocks remain stable for a certain period after being subjected to dynamic disturbances (blasting, earthquakes, vibration waves, *etc.*). However, the microscopic crack damage caused by these dynamic disturbances accumulates within the rock, and the local stress environment changes. The larger the disturbance energy and the more frequent the disturbances, the greater the accumulation of crack damage within the rock. When the damage accumulates to a certain extent, the rock mass becomes unstable, potentially triggering rockbursts. According to the analysis of time-delayed rockburst cases, *in-situ* stress, structural planes, and dynamic disturbances are key influencing factors.

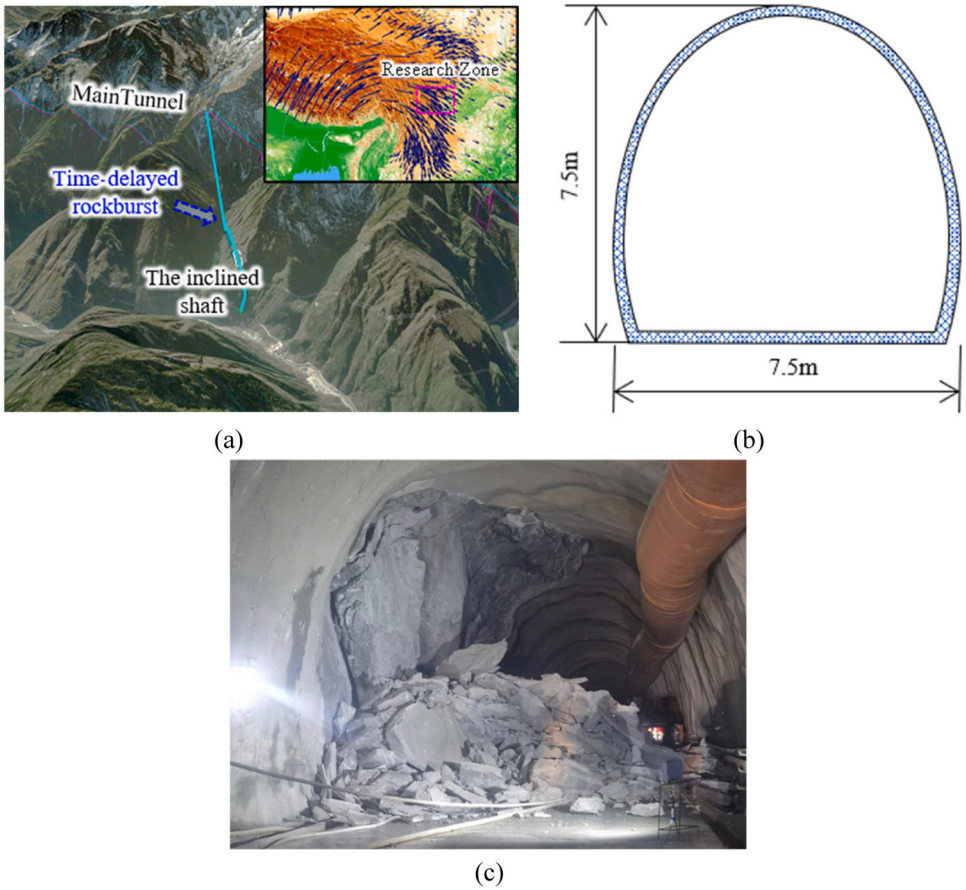

Fig. 2. Engineering geological conditions of the research zone: (a) topography near the inclined shaft project; (b) cross- section of the tunnel; (c) photograph of the extremely intensive rockburst.

3.1. *In-situ stress*

In-situ stress is a crucial factor influencing time-delayed rockbursts. High *in-situ* stress and its differences (σ_1–σ_2, σ_2–σ_3) are potential and necessary conditions for rockburst occurrence. In underground construction projects such as tunnels, rock in areas of high *in-situ* stress may be in a critical stress state of creep failure [28]. High *in-situ* stress difference will increase the brittleness of the rock [24,27], raising the probability of rock instability and the possibility of rockbursts.

The area containing all the inclined shaft engineering should be selected to establish a 3D numerical model considering the topography, as shown in Fig. 3. The model has a length of 8250 m in the X direction, 6000 m in the Y direction, and a Z direction range from an elevation of −1000 m to the ground surface. Engineering practice has demonstrated that self-weight stress generated by the weight of the rock mass and tectonic stress generated by geological movements are the primary factors influencing the formation of the *in-situ* stress field. The self-weight of the rock mass and geological movement are chosen as the primary factors for the *in-situ* stress regression analysis, including horizontal compressive stress and horizontal shear stress. Using FLAC3D software, displacement is applied to the boundary surfaces of the model to simulate the tectonic stress formed by actual geological movements (Fig. 4).

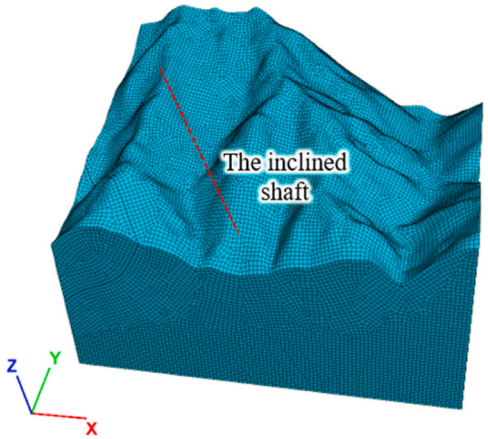

Fig. 3. Three-dimensional numerical meshes.

Based on the principle of multiple regression, the calculated *in-situ* stress values are taken as the dependent variable, while the stress values corresponding to the measured points for the gravitational stress field and tectonic stress field, obtained through numerical calculations, are treated as the independent variables. The form of the regression equation is then as follows:

$$\begin{vmatrix} \sum_{k=1}^{m}\sum_{j=1}^{6}(\sigma_{jk}^{1})^2 & \sum_{j=1}^{m}\sum_{j=1}^{6}\sigma_{jk}^{1}\sigma_{jk}^{2} & \cdots & \sum_{k=1}^{m}\sum_{j=1}^{6}\sigma_{jk}^{1}\sigma_{jk}^{n} \\ & \sum_{k=1}^{m}\sum_{j=1}^{6}(\sigma_{jk}^{1})^2 & \cdots & \sum_{k=1}^{m}\sum_{j=1}^{6}\sigma_{jk}^{2}\sigma_{jk}^{n} \\ & \vdots & \vdots & \vdots \\ \text{Symmetric} & & & \sum_{k=1}^{m}\sum_{j=1}^{6}(\sigma_{jk}^{1})^2 \end{vmatrix} \times \begin{vmatrix} b_1 \\ b_2 \\ \vdots \\ b_n \end{vmatrix} = \begin{vmatrix} \sum_{k=1}^{m}\sum_{j=1}^{6}\sigma_{jk}^{1}\sigma_{jk} \\ \sum_{k=1}^{m}\sum_{j=1}^{6}\sigma_{jk}^{2}\sigma_{jk} \\ \vdots \\ \sum_{k=1}^{m}\sum_{j=1}^{6}\sigma_{jk}^{n}\sigma_{jk} \end{vmatrix} \quad (1)$$

In the equation, represents the j observed stress component at the k observation point, and represents the numerical calculated stress

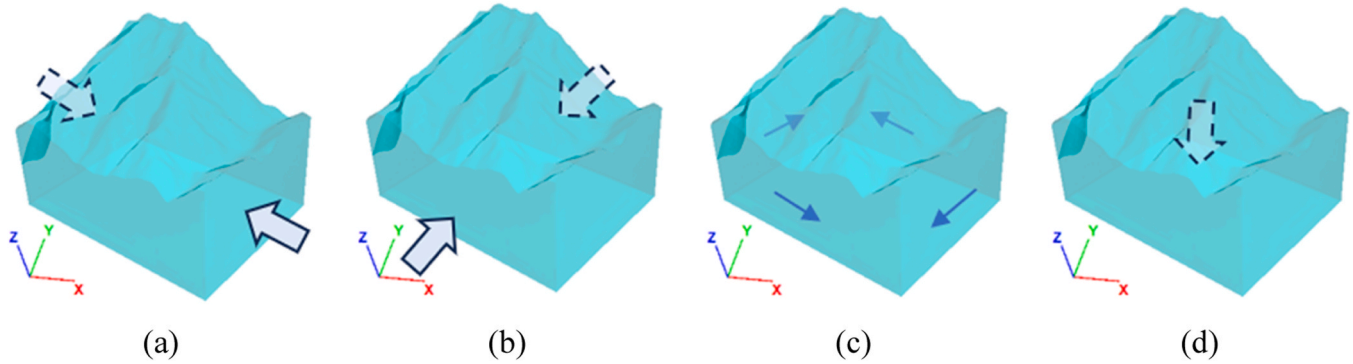

Fig. 4. Schematic diagrams showing how the tectonic action is modeled: (a) compression in the *x*-direction; (b) compression in the *y*-direction; (c) shearing action in the horizontal *x*-*y* plane; (d) gravity.

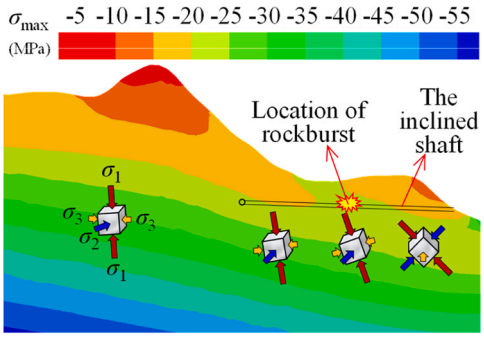

Fig. 5. Distribution of the maximum principal stress in the inclined shaft (after He et al.[11].

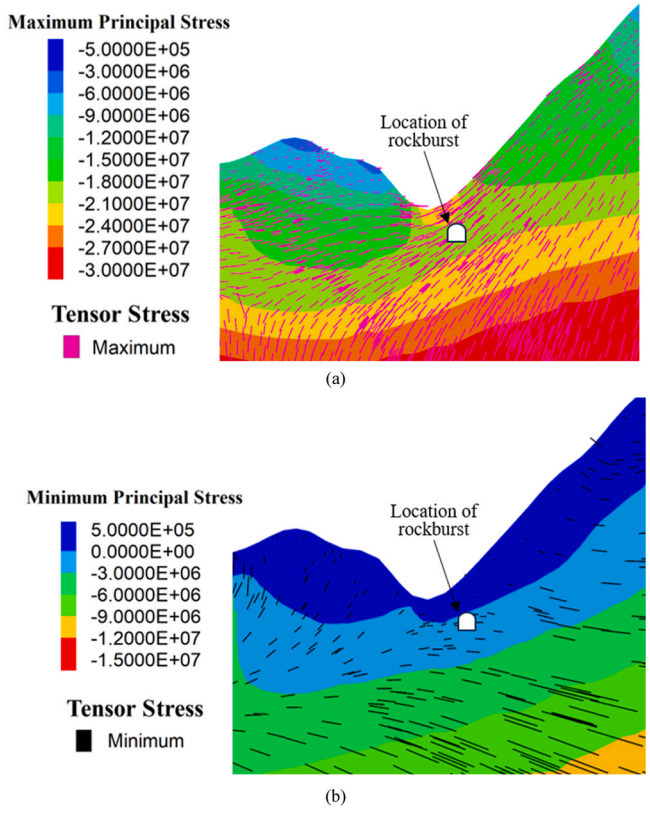

Fig. 6. Principal stress distribution profiles of extremely intensive rockburst: (a) the distribution and direction of maximum principal stress in Pa; (b) the distribution and direction of minimum principal stress in Pa.

component at the *k* observation point under the *i* condition. correspond to the 6 stress components. According to the least squares method, the sum of *Q* squared residuals is minimized. By solving this system of equations, the unknown regression coefficients are obtained. Thus, the regression *in-situ* stress at any point within the calculation area can be obtained from Eq. (1).

Based on the results of the *in-situ* stress field inversion, the inclined shaft is located in a typical valley stress field area (Fig. 5). The maximum principal stress direction is distributed along the slope (Fig. 6a). The maximum principal stress value reaches up to 20 MPa. Although the tunnel depth is only about 280 m, the tunnel is located in the stress concentration area within the valley stress field, which the maximum principal stress along with the slope around the tunnel is equivalent to the self-weight stress at a depth of 750 m. The minimum principal stress direction is perpendicular to the slope, with a value as low as 3 MPa (Fig. 6b), which is only 0.15 times the maximum principal stress. The minimum principal stress direction is near-perpendicular to the slope, corresponding to the unloading direction within the slope. The minimum principal stress is equivalent to the self-weight stress at a depth of 200 m. In the typical valley stress field, the tunnel is located in the zone of stress concentration. The maximum principal stress is abnormally high, and there is a significant difference between the maximum and minimum principal stresses.

Based on the original *in-situ* stress field, the tunnel excavation simulation was conducted, and the contour of the maximum principal stress near the "9.21" rockburst was extracted (Fig. 7). It is evident that, after excavation, stress concentration occurred at both the left hance and the right arch foot, with the maximum principal stress at the left arch shoulder being approximately 40 ~ 50 MPa.

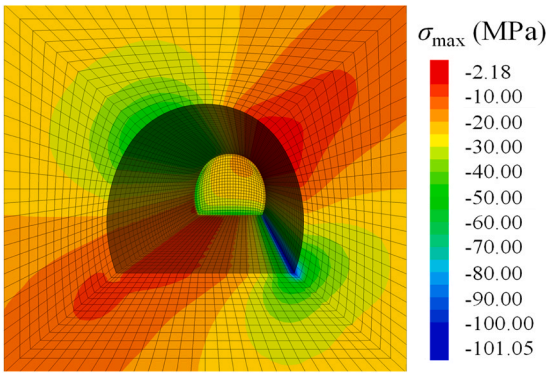

Fig. 7. The maximum principal stress distribution of tunnel cross-section at the rockburst location.

(a) (b)

Fig. 8. Structure-controlled rockbursts: (a) strain-structural plane slip rockburst; (b) fault-slip rockburst.

Fig. 9. Structural planes in the extremely intensive time-delayed rockburst.

3.2. Structural planes

The primary structural planes such as joints, fractures, and interlayers are abundant in most time-delayed rockburst areas. During the stress adjustment associated with tunnel excavation, failure tends to propagate along these structural planes. When numerous primary structural planes extend, intersect, and penetrate, greater intensity time-delayed rockbursts usually occur [29]. The rockburst primarily produces wedge-shaped blocks that are relatively large, with thicknesses typically ranging from 0.4 m ~ 0.8 m. The failure is dominated by expansion and slip along the structural plane.

During the excavation process, the regions where strain-structural plane slip rockbursts or fault-slip rockbursts occur have a higher risk of subsequent time-delayed rockburst disasters. Rockbursts caused by fault sliding or shear fracturing can lead to stress concentration during blasting construction disturbance, resulting in dynamic failure and shear slip instability along the weak structural planes under external load. The frequency of time-delayed rockbursts is relatively high in such conditions. Strain-structural plane slip rockbursts controlled by multiple sets of structural planes are illustrated in Fig. 8a; Fig. 8b demonstrates a fault-slip rockburst.

The area containing the "9.21" time-delayed extremely intensive rockburst is characterized by multiple intersecting structural planes and well-developed joints. The rockburst pit of the time-delayed rockburst reveals multiple structural planes, with shear slip phenomena observed near these planes. The boundaries of the rockburst pit are controlled by the structural planes, and the failure occurs along them. The failure mechanism is characterized as a strain-structure slip rockburst. Exposed structural planes are distributed at the initial and terminal positions of the rockburst (Fig. 9).

3.3. Dynamic disturbance

During tunnel construction, surrounding rock is subjected to various forms of vibrational disturbances: drilling and blasting tunnel excavation frequently disturbs the rock with blasting stress waves, while tunnels in earthquake belt areas are often affected by seismic waves. Dynamic disturbance can accelerate the deformation of the surrounding rock, disrupt the stress equilibrium of the rock mass, and induce secondary stress concentration. For the rock masses containing structural planes, the propagation process of blast stress waves or seismic waves

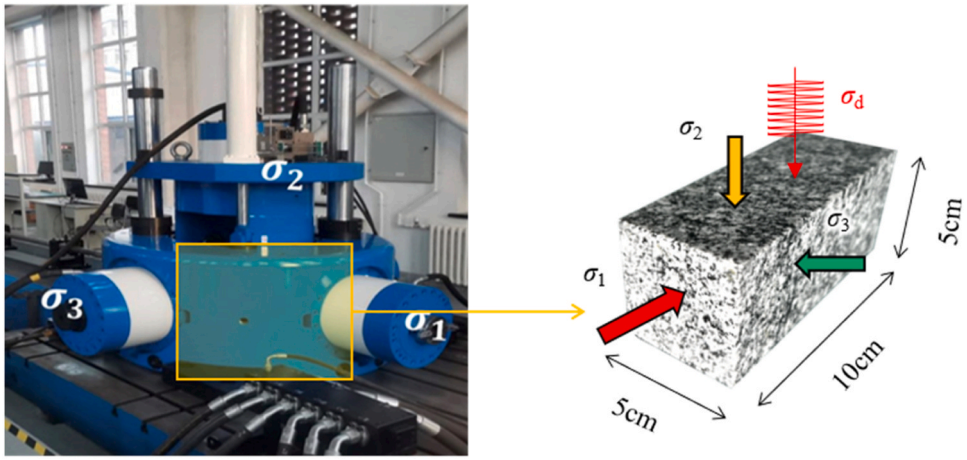

Fig. 10. The dynamic disturbance true triaxial compression testing system.

can lead to the extension of preexisting fissures and the generation of numerous new fissures. After a long period of stress adjustment and dynamic disturbances, joints and fissures in rock masses with structural planes extend and coalesce. The sudden release of stored elastic strain energy after the surrounding rock reaches peak strength can result in rockbursts. To a certain extent, the risk of time-delay rockbursts will be greater when the surrounding rock is frequently disturbed by dynamic disturbance and contains multiple structural planes.

3.3.1. *Long-term dynamic disturbance laboratory testing*

Different from the immediate rockbursts, time-delayed rockbursts exhibit a certain time delay. The failure does not occur immediately, instead, energy is suddenly released after the stress accumulates to a certain threshold, causing the rock mass to collapse. Investigating the mechanisms of action of time-delayed rockbursts is crucial for the safe design of deep excavation work. The better to understand this phenomenon, laboratory tests simulating various stress conditions were conducted to reveal the mechanisms underpinning, and factors affecting, time-delayed rockbursts (limited by the power consumption of the testing machine, the long-term dynamic disturbance loading method described herein is: dynamic disturbance + long-term holding stress application).

The rock samples from the "9.21" time-delayed extremely intensive rockburst were collected on-site and processed into rectangular prisms with dimensions of 5 cm (length) × 5 cm (width) × 10 cm (height), with a perpendicularity tolerance within 0.02 mm, as shown in Fig. 10. The experiments were conducted using the high-pressure hard rock wide-frequency low-amplitude surface disturbance rigid true triaxial testing apparatus developed by Northeastern University [7]. The testing apparatus consists of a rigid base, a horizontal rigid frame, and a vertical rigid frame, with a frame stiffness greater than 25 GPa. The maximum loading pressure in the horizontal direction is 3000 kN, and in the vertical

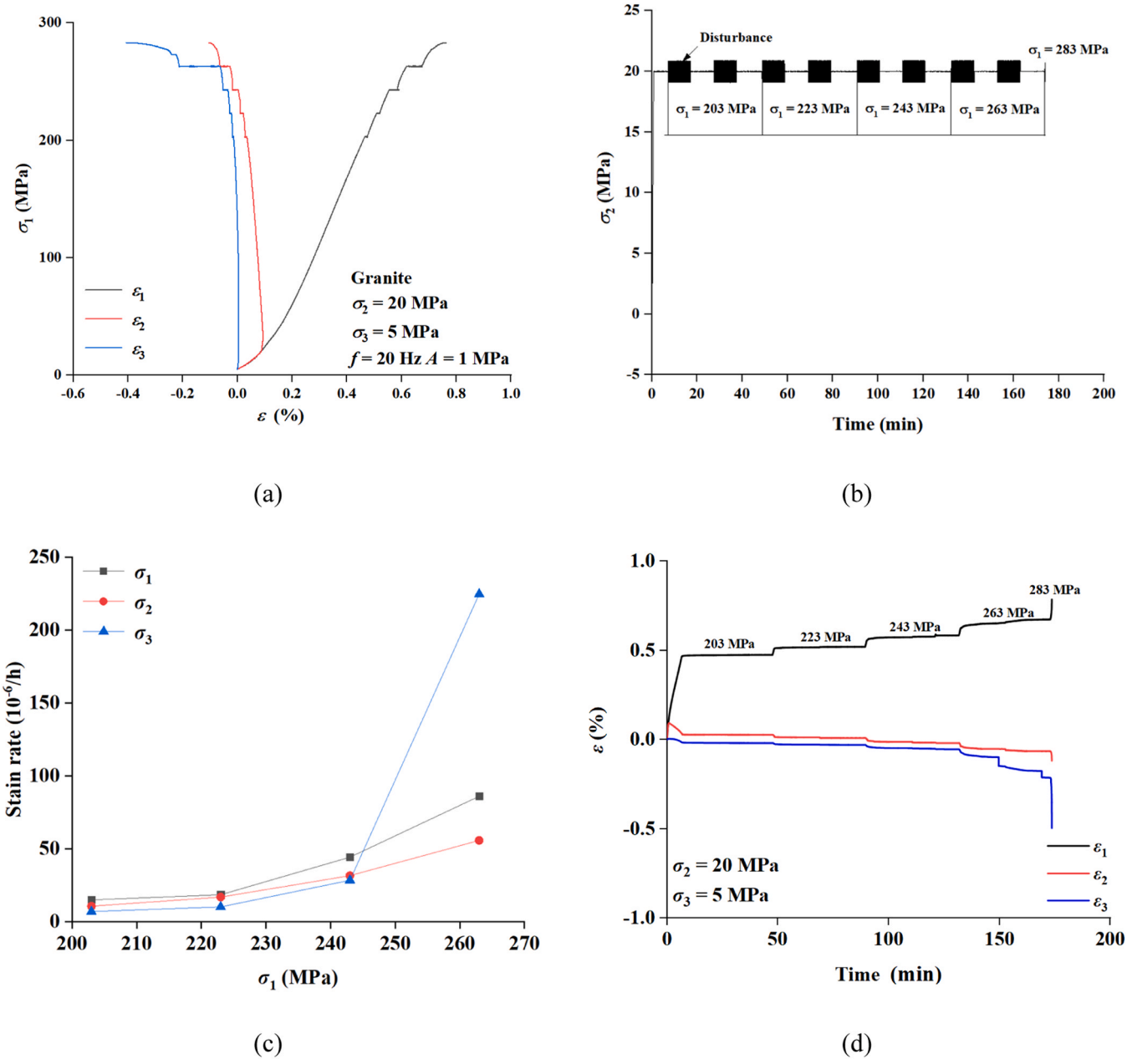

Fig. 11. True triaxial stress-strain curve under long-term dynamic disturbance loading: (a) true triaxial stress-strain curves of granite; (b) schematic of disturbance time and applied disturbance stress; (c) principal stress-creep rate; (d) time *versus* strain.

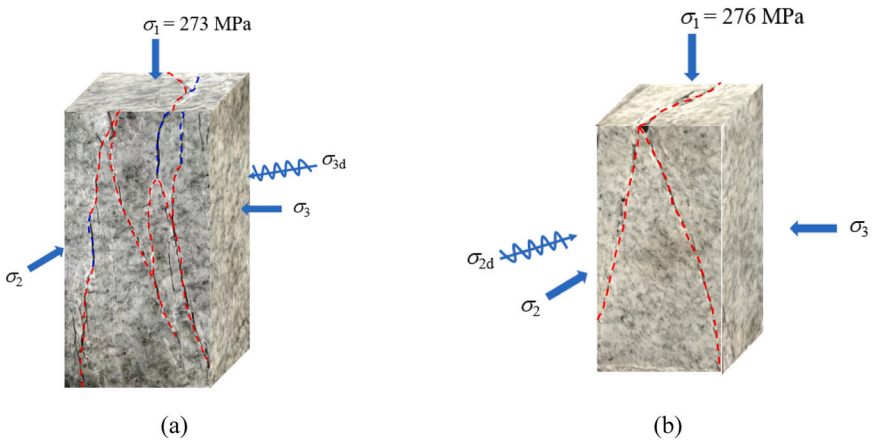

Fig. 12. Long-term dynamic disturbance loading on rock fracture patterns: (a) dynamic disturbances in the σ_3 direction; (b) dynamic disturbances in the σ_2 direction.

Table 2
Earthquake event statistics after tunnel excavation to trigger a time-delayed extremely intensive rockburst.

Serial No.	Date	Magnitude	Latitude	Longitude	Depth (km)	Location
1	2022.05.20	4.8	29.67	102.48	20	Hanyuan County, Ya'an City, Sichuan
2	2022.09.05	2.8	29.51	102.11	8	Luding County, Ganzi Prefecture, Sichuan
3	2022.09.05	3.1	29.61	102.04	9	Luding County, Ganzi Prefecture, Sichuan
4	2022.09.05	3.2	29.58	102.06	12	Luding County, Ganzi Prefecture, Sichuan
5	2022.09.05	6.8	29.59	102.08	16	Luding County, Ganzi Prefecture, Sichuan
6	2022.09.06	3.1	29.64	102.07	11	Luding County, Ganzi Prefecture, Sichuan
7	2022.09.06	3.2	29.61	102.01	8	Luding County, Ganzi Prefecture, Sichuan
8	2022.09.07	2.9	29.67	102.06	10	Luding County, Ganzi Prefecture, Sichuan
9	2022.09.07	3	29.5	102.2	12	Luding County, Ganzi Prefecture, Sichuan
10	2022.09.08	3.3	29.78	102.01	10	Luding County, Ganzi Prefecture, Sichuan

direction, it is 2000 kN. Both static and disturbance loads can be independently applied in the vertical direction.

As shown in Fig. 11a, the complete stress-strain curve of granite under long-term dynamic disturbance stress is presented at static stress levels: $\sigma_2 = 5$ MPa and $\sigma_3 = 20$ MPa. The dynamic disturbance parameters are set to: $f = 20$ Hz and $A = 1$ MPa. Fig. 11b depicts the stress changes during the dynamic disturbance applied in the experiment, with each step lasting 40 min, consisting of dynamic disturbance stress application for 20 min and static stress holding for 20 min. Fig. 11c presents the variations in strain rates along the three principal stress directions with the increase in the principal stresses during long-term dynamic disturbance loading. The strain rates in all three directions are found to gradually increase, indicating that the internal microcracks in the rock expand progressively with long-term dynamic disturbance, leading to the significant process of rock damage accumulation. At the final stage ($\sigma_1 = 283$ MPa), the rapid increase in the minimum principal strain rate is the primary cause of the sudden rock fracture. Fig. 11d illustrates the variation of strain over time in the three principal stress directions. It is evident that, in the maximum principal stress direction, strain does not significantly increase over time. The minimum principal stress remains aligned in the direction with the most noticeable strain variation. In deep tunnels, the minimum stress direction is often radial, correlating with the occurrence of time-delayed rockburst events, which are typically initiated in a radial direction, such as at the tunnel vault and sidewalls. This corresponds to the minimum principal stress direction of a time-delayed rockburst.

Fig. 12 illustrates the typical failure modes of rocks under two types of long-term dynamic disturbance true triaxial tests. It can be observed that dynamic disturbances in the σ_3 direction promote tensile failure, while those in the σ_2 direction promote shear failure. This explains why dynamic disturbances in the σ_3 direction exert a greater influence on the peak performance of rocks compared to those in the σ_2 direction. Based on field observations, long-term dynamic disturbance along the tunnel axis predominantly leads to time-delayed rockbursts characterized by shear cracking. Conversely, long-term dynamic disturbance in the radial direction of the tunnel (adjacent tunnel TBM excavation and similar conditions generate long-term dynamic disturbances in the σ_3 direction) primarily results in time-delayed rockbursts characterized by tensile cracking.

3.3.2. *Multi-earthquake disturbances*

The location of the "9.21" rockburst is characterized by two distinct zones trending NE and NW: aftershock zones of the Wenchuan-Lushan earthquake sequence in Qingchuan-Ya'an-Luding, and small earthquake belt along the Xianshuihe-Zemuhe-Anninghe fault zone in Luhuo-Kangding-Shimian. After tunnel excavation and before the "9.21" rockburst, 10 earthquakes with $M \geq 2.8$ were recorded (Table 2).

According to the historical earthquake statistics from the China earthquake network, a 6.8 magnitude earthquake occurred in Luding County, Ganzi Prefecture, Sichuan Province, on September 5, 2022. During the four days, Luding County experienced multiple aftershocks of around magnitude 3.0, and the "9.21" rockburst occurred about 35 km from the epicenter of the Luding, Sichuan earthquake.

3.3.3. *Blasting-induced vibration*

The vibration wave generated during blasting will affect the surrounding rock. Both numerical calculations and field microseismic monitoring indicated that blasting vibrations can trigger rockbursts around the underground opening at depth [30]. To investigate the influence of tunnel blasting construction on the surrounding rock of the excavated sections, blasting vibration sensors were arranged behind the tunnel face to monitor the vibration velocity, frequency, and duration during blasting (Fig. 13). Blasting vibration sensors were positioned at the stress-concentration area on the left arch shoulder of the tunnel, 214 m from the excavation face (Fig. 13a). The sensors and the sensor set-up method are depicted in Fig. 13b & c.

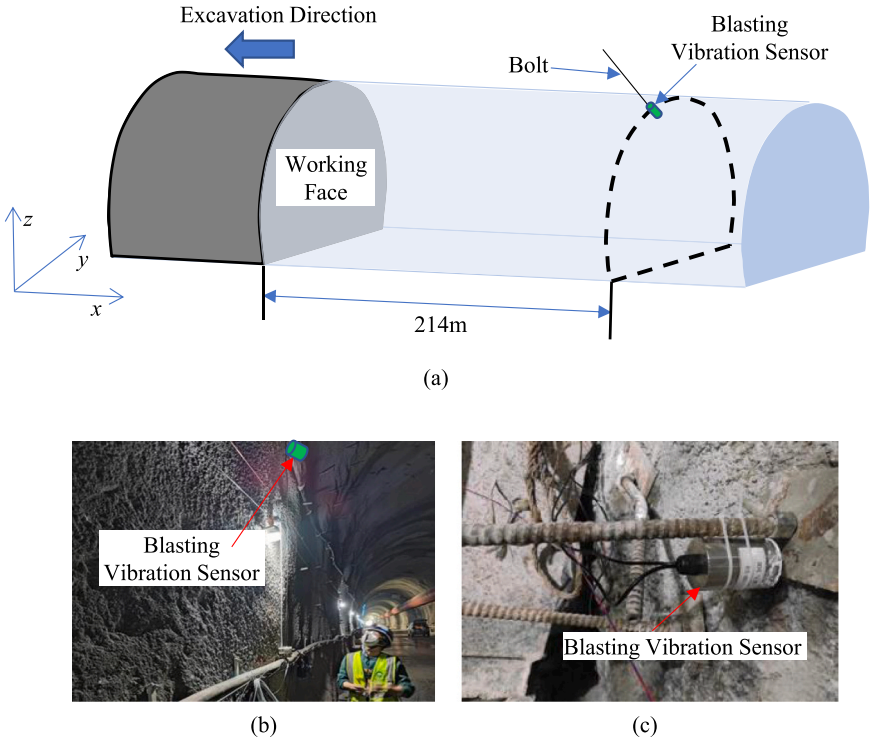

Fig. 13. Field monitoring of blasting vibration: (a) blasting vibration sensor layout; (b) on-site sensor installation; (c) sensor-fixed installation method.

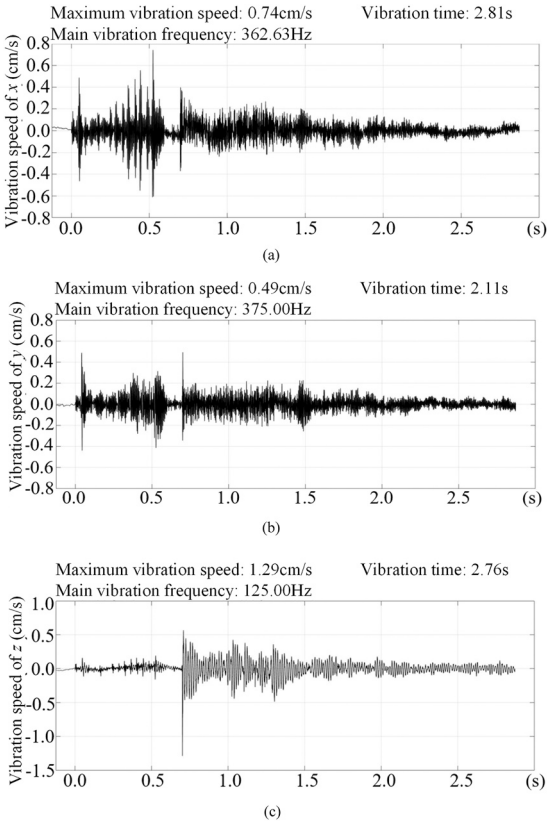

Fig. 14. Monitoring results of measured blasting vibration: (a) Blasting vibration velocity in the *x*-direction; (b) Blasting vibration velocity in the *y*-direction; (c) Blasting vibration velocity in the *z*-direction.

The measured blasting vibration data are shown in Fig. 14. With the maximum single charge of 88.50 kg and a total charge of 424.55 kg during excavation blasting, the vibration velocity at 214 m from the face ranged from 0.49 ~ 1.29 cm/s, with dominant frequencies between 125 ~ 375 Hz. The blasting vibration velocities were 0.74 cm/s in the *x*-direction, 0.49 cm/s in the *y*-direction, and 1.29 cm/s in the *z*-direction. The dominant frequencies were 362.63 Hz in the *x*-direction, 375 Hz in the *y*-direction, and 125 Hz in the *z*-direction.

4. Prevention and control of time-delayed rockburst

4.1. Principles of the energy control method

Rockburst occurs due to the sudden release of stored strain energy in surrounding rock. The surrounding rock at a certain depth has strong energy-storage capacity, and there is a zone where energy accumulates, slowly releases, then rapidly releases in an abrupt manner. When the fractured surrounding rock is in, or close to, the critical equilibrium state, it is prone to time-delayed rockburst under external disturbances such as those arising from seismic waves and blasting waves. According to the understanding of energy release characteristics in deep rock engineering, from the mechanical perspective, measures should be taken to enhance the energy storage capacity and ductility of the rock mass, while reducing the brittleness of rock mass, to avoid the sudden release of accumulated energy within the rock mass. The principles of the energy control method are shown in Fig. 15. To prevent disasters from the perspective of energy regulation, the following measures can be taken:

① Energy accumulation is reduced by optimizing the shape and size of excavation faces, the number and height of excavation steps, excavation rate, and parameters of guide tunnels such as location, shape, and size;

② Energy is pre-released and transferred by optimizing the position, length, and spacing of stress relief holes, along with measures such as pre-splitting the rock mass, to reduce the risk of sudden energy release;

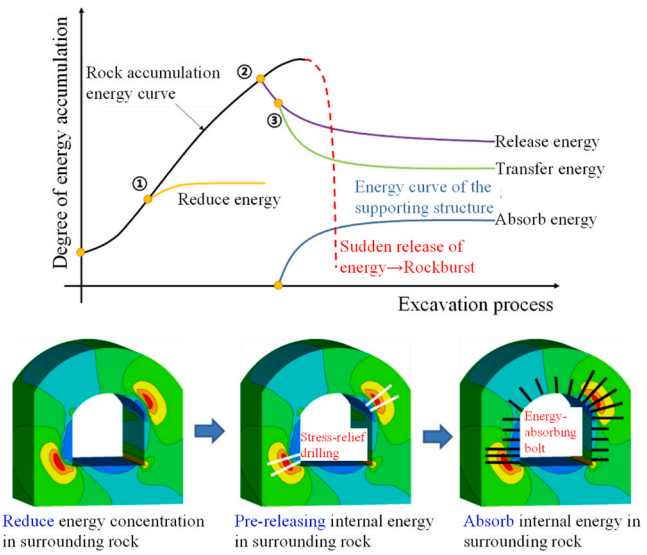

Fig. 15. Principles of the energy control method (after Feng [5]. Note: ① energy reduction; ② energy releasing; ③ energy absorption.

③ Energy is absorbed using support measures with certain energy absorption capabilities, such as energy-absorbed bolts, converting rock mass strain energy into support strain energy to reduce the degree of energy accumulation and its rate of release.

4.2. Energy control methods for time-delayed rockburst prevention

The principles of time-delayed rockburst prevention are illustrated in Fig. 16. For time-delayed rockbursts, in addition to energy-reduction measures taken during the design phase, the construction phase can also optimize the tunnel face blasting techniques (such as controlling the total amount of single blasting events or the maximum amount of explosives per blast, *etc.*); the wave-absorbing support materials can be used between the tunnel face and potential time-delayed rockburst area to minimize the influence of excavation disturbance on these areas, reduce the intensity and amplitude of stress adjustment, and mitigate energy concentration. In potential time-delayed rockburst areas, drill stress relief holes for pre-rereleasing stored elastic energy within the rock mass. It is necessary to install rock bolts for systematic and timeous use to reinforce the surrounding rock. Application of steel mesh and shotcrete are used to exert confining pressure on the surrounding rock, enhancing its strength and energy-storage capacity. Utilization of energy-absorbing supports to absorb some energy is essential.

4.3. Energy-absorbing and wave-absorbing support techniques

During the process of rockburst prevention and control, support measures should employ energy-absorbed bolts to control the fracture development and mitigate the ejection impact of surrounding rock. A stepwise decoupling energy-absorbed bolt with a simplified structure, as shown in Fig. 17, consists of threaded steel rod and stepwise decoupling isolation materials. The front end of the bolt rod is wrapped with stepwise decoupling materials to isolate the anchoring grout, while the threads (transverse ribs) still maintain partial engagement with the anchoring grout. However, the wrapping of the rod by the decoupling section may reduce the anchoring capacity of the bolt. When the anchoring strength is insufficient, for example, the bonding force between the remaining threaded segment of the bolt and the anchoring grout is lower than the breaking load of the rod, the bolt may slip. Therefore, the anchor head is installed at the tail end as an anchoring regulator to enhance the strength of the connection between the bolt and the anchoring grout. Multiple nuts can be added to the end of the bolt to

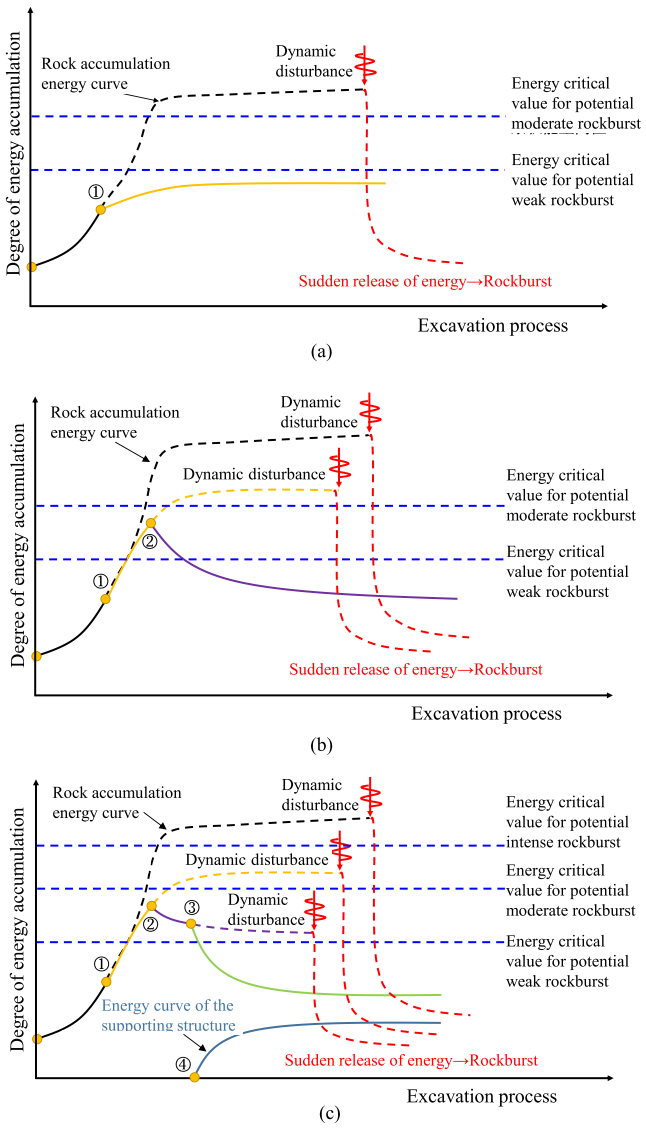

Fig. 16. Principles of time-delayed rockburst prevention and control: (a) Implementation of energy-reducing measures; (b) Implementation of energy-reducing and energy-releasing measures; (c) Implementation of energy-reducing, energy-releasing, and energy-absorbing measures (after Feng (2023)).

adjust the anchoring effect, ensuring that the anchoring force of the bolt is not lower than its breaking load.

The blasting excavation of the tunnel face, the blasting of the newly built tunnel and other blasting behaviors will cause the surrounding rock

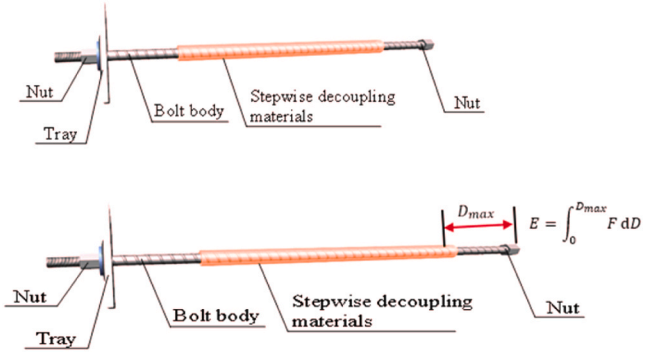

Fig. 17. A stepwise decoupling energy-absorbed bolt with a simplified structure.

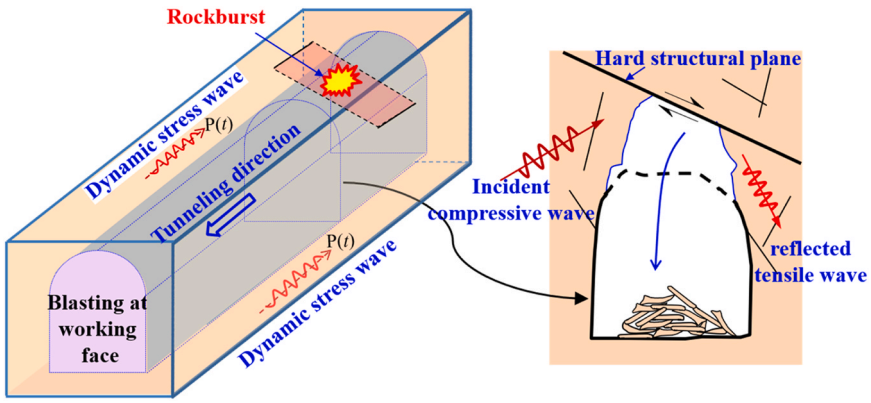

Fig. 18. Blast-induced rockburst in a previously excavated tunnel.

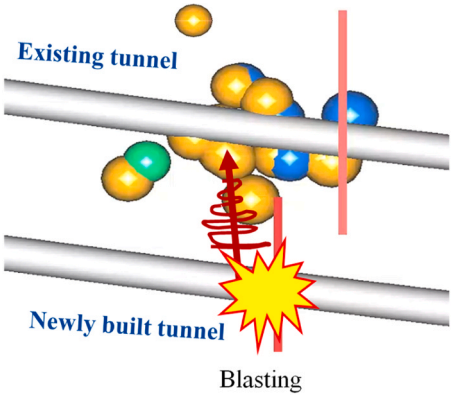

Fig. 19. The fracturing of the existing tunnel caused by the blasting of a new tunnel.

to break and damage (Fig. 18 & 19). During tunnel blasting, stress waves propagate through various media such as rock, structural planes, newly-generated cracks, and support materials. After excavation, immediate anchor shotcrete support is typically performed. When the anchor bolt holes are pressure-grouted, part of the anchoring material can permeate into the rock mass.

The stress wave propagation is affected by the surrounding rock, bolts, anchoring material, and the sprayed concrete on the rock surface (Fig. 20a). The propagation of stress waves in a medium is influenced by factors such as the type of medium, its thickness, and the angle of incidence. For longitudinal waves, assuming an elastic state, when the incident wave is perpendicular to the interface, both the refracted and reflected waves are longitudinal waves *P*. As shown in Fig. 20b, the *P* wave propagates from medium 1 to medium 2 and then further into medium 1, with the different media being parallel to each other. Assuming the initial stress wave *P* is σ_1, the wave impedances of medium 1 and medium 3 are $\rho_1 C_1$, and the wave impedance of medium 2 is $\rho_2 C_2$. R and T represent the reflection and transmission coefficients, respectively; n is the impedance ratio of the two media.

At the first interface:

$$n = \frac{\rho_{2C_2}}{\rho_1 C_1}$$

$$R_1 = \frac{\sigma_{R_1}}{\sigma_1} = \frac{n-1}{n+1} \tag{2}$$

$$T_1 = \frac{\sigma_{T_1}}{\sigma_1} = \frac{2}{n+1}$$

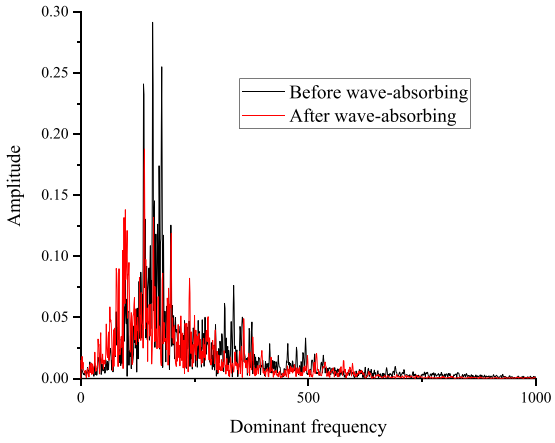

Fig. 21. Amplitude and dominant frequency characteristics of blasting disturbance wave before and after wave-absorption.

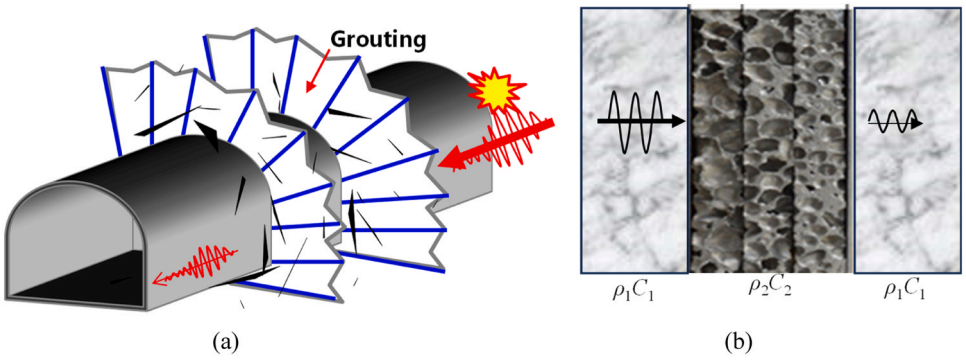

Fig. 20. Propagation of the blasting vibration stress wave: (a) schematic of wave-absorbed support; (b) schematic of stress wave propagation in multilayer media.

When $T1$ acts as the incident wave at the second interface, new transmission and reflection phenomena occur. Upon entering medium 3, T_1 becomes σ_{T2}, then [23]:

$$T_2 = \frac{\sigma_{T_2}}{\sigma_1} = \frac{4n}{(n+1)^2} \tag{3}$$

It can be observed that the smaller the wave impedance ratio, the higher the reflection coefficient and the lower the transmission coefficient, meaning the larger the longitudinal wave amplitude is weakened. Similar behavior was found with stress waves [19]. Therefore, in the selection of anchoring materials, the lower the wave impedance of the anchoring material, the more the energy borne by the stress wave is absorbed. The development and application of low-impedance materials in bolt groups, grout in surrounding rock, and shotcrete have the potential to absorb and attenuate stress waves transmitted to the tunnel face.

The field test of wave absorption was conducted in a tunnel in southwest China, and attenuation characteristics of disturbance wave after fast Fourier transform were obtained (Fig. 21). It can be observed that the amplitude of the blasting disturbance wave decreases from 0.29 *g* to 0.19 *g* (a reduction of 34.5 %); the dominant frequency decreases from 158 Hz to 140 Hz (a decrease of 11.4 %).

5. Conclusions

(1) Time-delayed rockbursts refer to rockbursts occurring in deep tunnels after stress readjustment and rebalancing following excavation unloading in high-stress areas, triggered by external dynamic disturbances. Time-delayed rockbursts are predominantly intense;
(2) *In-situ* stress, structural planes, and dynamic disturbances compose paramount factors influencing time-delayed rockbursts. High *in-situ* stress and its differences are essential conditions for their occurrence, while abundant structural planes and frequent dynamic disturbances increase the risk of time-delayed rockbursts;
(3) Time-delayed rockbursts abruptly release huge amounts of energy, which exhibit suddenness, randomness, and severe destructiveness. Simply increasing the strength of the support may be inefficient. A control approach should be adopted to reduce, pre-release, transfer, and absorb energy;
(4) Laboratory dynamic disturbance tests indicate that time-delayed rockburst occurrence requires long disturbance durations, compared to immediate rockbursts. Long-term, continuous, and multiple dynamic events will cause significant damage accumulation and formation of microcracks in hard rock;
(5) Long-term dynamic disturbances in the σ_3 direction primarily trigger tensile cracks in time-delayed rockbursts (associated with wave-induced stress from the tunnel face). In contrast, disturbances in the σ_2 direction mainly induce shear cracks (associated with wave-induced stress from adjacent tunnels).

CRediT authorship contribution statement

Xia-Ting Feng: Supervision, Resources, Project administration. **Zi-Hui Zhu:** Formal analysis. **Han-Yi Liu:** Validation, Investigation. **Heng-Yuan Zhang:** Visualization, Methodology. **Xiang-Rui Meng:** Software. **Ben-Guo He:** Writing – original draft, Funding acquisition, Conceptualization. **Hong-Pu Li:** Writing – original draft, Data curation.

Funding

This research was funded by the National Natural Science Foundation of China (Grant Nos. 52222810 and 52178383).

Declaration of Competing Interest

The author Xia-Ting Feng is Editor-in-Chief for Deep Resources Engineering and was not involved in the editorial review or the decision to publish this article. The other authors declare that they have no known competing financial interests or personal relationships that could have appeared to influence the work reported in this paper.

Acknowledgements

This work was supported by the National Natural Science Foundation of China (Grant Nos. 52222810 and 52178383).

References

[1] S. Akdag, M. Karakus, G.D. Nguyen, A. Taheri, Strain burst vulnerability criterion based on energy-release rate, Eng. Fract. Mech. 237 (2020) 107232, https://doi.org/10.1016/j.engfracmech.2020.107232.
[2] S. Akdag, M. Karakus, G.D. Nguyen, A. Taheri, T. Bruning, Evaluation of the propensity of strain burst in brittle granite based on post-peak energy analysis, Undergr. Space 6 (2021) 1–11, https://doi.org/10.1016/j.undsp.2019.08.002.
[3] M. Cai, Rockburst risk control and mitigation in deep mining, Deep Resour. Eng. 1 (2024) 100019, https://doi.org/10.1016/j.deepre.2024.100019.
[4] M. Cai, D. Champaigne, Influence of bolt-grout bonding on MCB conebolt performance, Int. J. Rock. Mech. Min. Sci. 49 (2012) 165–175.
[5] X.T. Feng, Mechanism, warning and dynamic control of rockburst development processes, Science Press, Beijing, 2013.
[6] X.T. Feng, B.R. Chen, S.J. Li, C.Q. Zhang, Y.X. Xiao, G.L. Feng, H. Zhou, S.L. Qiu, Z. N. Zhao, Y. Yu, D.F. Chen, H.J. Ming, Studies on the evolution process of rockbursts in deep tunnels, J. Rock. Mech. Geotech. Eng. 4 (2012) 289–295, https://doi.org/10.3724/SP.J.1235.2012.00289.
[7] X.T. Feng, M. Tian, C.X. Yang, B.G. He, A testing system to understand rock fracturing processes induced by different dynamic disturbances under true triaxial compression, J. Rock. Mech. Geotech. Eng. 15 (2023) 102–118, https://doi.org/10.1016/j.jrmge.2022.02.002.
[8] Feng, X.T., Xiao, Y.S., Feng, G.L., 2012b. Mechanism, Warning And Dynamic Control Of Rockburst Evolution Process, in: ISRM International Symposium-Asian Rock Mechanics Symposium. ISRM, p. ISRM-ARMS7.
[9] X.T. Feng, C.X. Yang. Hard Rock Mechanics in Deep Engineering, Science Press, Beijing, 2023.
[10] X.T. Feng, C.X. Yang, B.G. He, Z.B. Yao, L. Hu, W. Zhang, R. Kong, J. Zhao, Z.B. Liu, X. Bi, Artificial intelligence technology in rock mechanics and rock engineering, Deep Resour. Eng. 1 (2024) 100008, https://doi.org/10.1016/j.deepre.2024.100008.
[11] B.G. He, H.P. Li, X.T. Feng, X.R. Meng, Estimating the complete in-situ stress tensor along deep tunnels with frequent rockbursts near a steep valley, Bull. Eng. Geol. Environ. 83 (1) (2023), https://doi.org/10.1007/s10064-023-03497-6.
[12] M.C. He, W.L. Gong, J. Wang, P. Qi, Z.G. Tao, S. Du, Y.Y. Peng, Development of a novel energy-absorbing bolt with extraordinarily large elongation and constant resistance, Int. J. Rock. Mech. Min. Sci. 67 (2014) 29–42.
[13] M.C. He, F.Q. Ren, D.Q. Liu, Rockburst mechanism research and its control (SI: Dynamic failure in rock masses), Int. J. Min. Sci. Technol. 28 (2018) 829–837, https://doi.org/10.1016/j.ijmst.2018.09.002.
[14] A. Keneti, B.A. Sainsbury, Review of published rockburst events and their contributing factors, Eng. Geol. 246 (2018) 361–373, https://doi.org/10.1016/j.enggeo.2018.10.005.
[15] J.P. Liu, X.T. Feng, Y.H. Li, Y. Sheng, Studies on temporal and spatial variation of microseismic activities in a deep metal mine, Int. J. Rock. Mech. Min. Sci. 60 (2013) 171–179.
[16] T.H. Ma, C.A. Tang, S.B. Tang, L. Kuang, Q. Yu, D.Q. Kong, X. Zhu, Rockburst mechanism and prediction based on microseismic monitoring, Int. J. Rock. Mech. Min. Sci. 110 (2018) 177–188.
[17] A.M. Naji, M.Z. Emad, H. Rehman, H. Yoo, Probabilistic analysis of shear strength of intact rock in triaxial compression: a case study of Jinping II project, Tunn. Undergr. Space Technol. 111 (2019) 2115–2130, https://doi.org/10.1016/j.tust.2018.11.009.
[18] P.Z. Pan, F.Y. Tan, F.Q. Li, F.D. Chi, X.F. Liu, Z.F. Wang, A three-dimensional numerical study on the stability of layered rock spillway tunnels in alpine canyon areas, Deep Resour. Eng. 1 (2024) 100023, https://doi.org/10.1016/j.deepre.2024.100023.
[19] Pao, Y.H., Mow, C.C., Achenbach, J.D., 1973. Diffraction of Elastic Waves and Dynamic Stress Concentrations.
[20] R. Shirani Faradonbeh, S. Shaffiee Haghshenas, A. Taheri, R. Mikaeil, Application of self-organizing map and fuzzy c-mean techniques for rockburst clustering in deep underground projects, Neural Comput. Appl. 32 (2020) 8545–8559, https://doi.org/10.1007/s00521-019-04353-z.
[21] R. Shirani Faradonbeh, A. Taheri, L. Ribeiro e Sousa, M. Karakus, Rockburst assessment in deep geotechnical conditions using true-triaxial tests and data-driven approaches, Int. J. Rock. Mech. Min. Sci. 128 (2020) 104279, https://doi.org/10.1016/j.ijrmms.2020.104279.

[22] G.S. Su, X.T. Feng, J.H. Wang, J.Q. Jiang, L.H. Hu, Experimental study of remotely triggered rockburst induced by a tunnel axial dynamic disturbance under true-triaxial conditions, Rock. Mech. Rock. Eng. 50 (2017) 2207–2226, https://doi.org/10.1007/s00603-017-1218-y.
[23] J.W. Tedesco, D.W. Landis, Wave propagation through layered systems, Comput. Struct. 32 (1989) 625–638, https://doi.org/10.1016/0045-7949(89)90351-9.
[24] N. Trinh, K. Jonsson, Design considerations for an underground room in a hard rock subjected to a high horizontal stress field at Rana Gruber, Norway, Tunn. Undergr. Space Technol. 38 (2013) 205–212, https://doi.org/10.1016/j.tust.2013.07.006.
[25] L. Weng, L.Q. Huang, A. Taheri, X.B. Li, Rockburst characteristics and numerical simulation based on a strain energy density index: a case study of a roadway in Linglong gold mine, China, Tunn. Undergr. Space Technol. 69 (2017) 223–232, https://doi.org/10.1016/j.tust.2017.05.011.
[26] S.C. Zhang, T.H. Ma, C.A. Tang, P. Jia, Y.C. Wang, Microseismic monitoring and experimental study on mechanism of delayed rockburst in deep-buried tunnels, Rock. Mech. Rock. Eng. 53 (2020) 2771–2788, https://doi.org/10.1007/s00603-020-02069-4.
[27] Y. Zhang, X.T. Feng, C.X. Yang, Q. Han, Z.F. Wang, R. Kong, Evaluation method of rock brittleness under true triaxial stress states based on pre-peak deformation characteristic and post-peak energy evolution, Rock. Mech. Rock. Eng. 54 (2021) 1277–1291, https://doi.org/10.1007/s00603-020-02330-w.
[28] J. Zhao, X.T. Feng, C.X. Yang, Y.Y. Zhou, Y. Zhang, Study on time-dependent fracturing behaviour for three different hard rock under high true triaxial stress, Rock. Mech. Rock. Eng. 54 (2021) 1239–1255, https://doi.org/10.1007/s00603-020-02327-5.
[29] H. Zhou, F.Z. Meng, C.Q. Zhang, D.W. Hu, F.J. Yang, J.J. Lu, Analysis of rockburst mechanisms induced by structural planes in deep tunnels, Bull. Eng. Geol. Environ. 74 (2015) 1435–1451, https://doi.org/10.1007/s10064-014-0696-3.
[30] W.C. Zhu, Z.H. Li, L. Zhu, C.A. Tang, Numerical simulation on rockburst of underground opening triggered by dynamic disturbance, Tunn. Undergr. Space Technol. 25 (2010) 587–599, https://doi.org/10.1016/j.tust.2010.04.004.

Prof. Ben-Guo He received his Ph.D degree at Southwest Jiaotong University, China in 2013. From 2014–2017, he was a Postdoc Research Fellow in Department of Earth and Environmental Sciences, Ben-Gurion University of the Negev. He took the positions of associate professor and professor at Northeastern University, China. He works at Northeastern University, China, as vice dean of the Institute of Deep Engineering and Intelligent Technology. He has presided over 10 projects, including Israel PBC scholarship program for outstanding post-doctoral students, Outstanding Youth Science Foundation of China, sub-projects of National Key Research and Development Program (the accumulated national research funds exceeds 2 million dollars). Moreover, Prof. He is a member of International Society for Rock Mechanics and Rock Engineering (ISRM) Commission on Design Methodology. He has published more than 60 papers along with 18 invention patents. His research interests cover rockburst, monitoring, and rock mechanics applied in deep engineering.